Probing the Chemistries of the Substrate and Flavin Ring System of *p*-Hydroxybenzoate Hydroxylase by Raman Difference Spectroscopy[†]

John Clarkson,[‡] Bruce A. Palfey,[§] and Paul R. Carey*[,‡]

Department of Biochemistry, Case Western Reserve University, 10900 Euclid Avenue, Cleveland, Ohio 44106-4935, and Department of Biological Chemistry, University of Michigan Medical School, Ann Arbor, Michigan 48109-0606

Received June 25, 1997; Revised Manuscript Received August 8, 1997[⊗]

ABSTRACT: Details of the substrate, *p*-hydroxybenzoate, and substrate analog, *p*-aminobenzoate, binding to *p*-hydroxybenzoate hydroxylase have been elicited by Raman difference spectroscopy. Deep red (752 nm) excitation was used to avoid interference from a fluorescence background. The Raman data provide information on changes in the ligand upon binding as well as changes in the flavin ring system of the enzyme in the enzyme−substrate complex. For *p*-aminobenzoate, its three most intense Raman features, due to a phenyl mode (1607 cm^{-1}) and carboxylate stretching (1383 cm^{-1}) and scissoring (863 cm^{-1}) motions, are little perturbed upon binding and show no changes in the pH range 6.5−8.5. However, changes in a number of spectral features associated with isoalloxazine modes in this pH range are evidence for a protonation/deprotonation event occurring in or near the active site. A feature in the difference spectrum of the complex at 1700 cm^{-1} is assigned to the stretch of the 4C═O group of the isoalloxazine; the relatively narrow profile of this feature is due to the ring being held in a rigid network of hydrogen bonds as demonstrated by the X-ray-derived structure [Schreuder, H. A., Prick, P. A. J., Wierenga, R. K., Vriend, G., Wilson, K. S., Hol, W. G. J., & Drenth, J. (1989) *J. Mol. Biol. 208*, 679−696]. The absence of a corresponding negative band in the spectrum near 1725 cm^{-1} shows that in the enzyme, in the absence of ligand, the 4C═O peak is "washed out" by a fluctuating series of hydrogen bonds to water molecules which penetrate to the flavin ring, resulting in a broad C═O stretching feature which escapes detection in the difference spectrum. For *p*-hydroxybenzoate, upon complexation, the $-COO^-$ symmetric stretch shifts 10 cm^{-1}, which is ascribed to the formation of the salt bridge to the guanidinium of Arg 214, seen in the X-ray structure. This is in contrast with the results for the complex involving the *p*-amino analog where no shift in the carboxylate mode is detected and demonstrates an advantage of using vibrational spectroscopy as a fine probe of active site interactions, since the X-ray structures for the *p*-amino and *p*-hydroxy analog complexes indicate that the structures in the $-COO^-$ group guanidinium regions are the same. The Raman difference data for the substrate complex in the 1700 cm^{-1} region closely resemble those for the *p*-amino analog, indicating that in both cases the 4C═O group is participating in a rigid hydrogen bonding network in the complexes with ligand but is in a more dynamic hydrogen bonding environment involving water molecules in the unliganded enzyme. In order to measure the pK_a of the −OH group in bound *p*-hydroxybenzoate, the substrate was labeled with ^{18}O in both $-COO^-$ oxygen atoms. By subtracting the Raman spectrum of the complex with labeled substrate from that with unlabeled substrate, a simple difference spectrum was obtained with features involving the $-COO^-$ group alone. These features were used to measure the pK_a of the ring hydroxyl group which was found to be 8.3. The value determined from absorption spectroscopy is 7.4, and possible reasons for the discrepancy are discussed. Both methods are in accord, however, in that they show that the pK_a of the bound substrate is substantially below that for the free, a device which assists in the hydroxylation at the 3-position.

The hydroxylation of many activated aromatic compounds by bacteria is accomplished by a family of enzymes that utilize FAD as a nondissociable prosthetic group. Molecular oxygen is the source of the hydroxyl group, and water is a byproduct. Catalysis by the flavoprotein hydroxylases occurs through a reductive and oxidative half-reaction. The most extensively studied flavoprotein hydroxylase is *p*-hydroxybenzoate hydroxylase (PHBH),[1] a dimeric enzyme, 45 kDa per subunit, that converts *p*-hydroxybenzoate (*p*OHB) to 3,4-dihydroxybenzoate [see (*1*) for a review]. A number of reaction intermediates have been observed when *p*OHB or substrate analogs are hydroxylated. The key intermediate in the reaction is the flavin C4a-hydroperoxide, which is formed when O_2 reacts with the reduced flavin. The flavin hydroperoxide is a potent electrophile and transfers the distal oxygen atom to the 3-position of the substrate in an electrophilic aromatic substitution reaction. It is thought that the enzyme accelerates this reaction by lowering the phenolic pK_a of *p*OHB (*2*, *3*); the phenolate form of the substrate is a better nucleophile for attacking the distal oxygen of the flavin hydroperoxide (*4*). Supporting this are experiments with site-directed mutants, which have demonstrated that

[†] B.A.P. was supported by U.S. Public Health Service Grants GM 20877 to David P. Ballou and GM 11106 to Vincent Massey.

* To whom correspondence should be addressed. Fax: 216 368 4544. Telephone: 216 368 0031. E-mail: carey@biochemistry.cwru.edu.

[‡] Case Western Reserve University.

[§] University of Michigan Medical School.

[⊗] Abstract published in *Advance ACS Abstracts,* October 1, 1997.

[1] Abbreviations: *p*OHB, *p*-hydroxybenzoate; *p*ABA, *p*-aminobenzoate; PHBH, *p*-hydroxybenzoate hydroxylase; Tris, tris(hydroxymethyl)aminomethane.

S0006-2960(97)01527-4 CCC: $14.00

mutations with an impaired ability to ionize pOHB also hydroxylate the substrate slowly or not at all (*3, 5, 6*).

PHBH has been studied extensively by X-ray diffraction (*7, 8, 9, 10, 11, 12*). Structures show that the flavin and aromatic substrate are ideally positioned for the reaction of the C4a-hydroperoxide with the 3-position of the aromatic substrate (*13*). The area near the reactive site is inaccessible to solvent, a feature that prevents H_2O_2 from eliminating from the reactive flavin hydroperoxide. A network of hydrogen bonds to the phenolic group of *p*OHB has been inferred from crystallographic data (*7*), and the residues involved in this network have been identified as being important in lowering the phenolic pK_a of *p*OHB (*3; 5*). The chemistry of the flavin is also modulated by interactions with the protein; for instance, the redox potential of the isoalloxazine is ∼50 mV higher than that of free FAD (*3*). Thus, it is clear that the protein acts to direct the chemical events of PHBH catalysis, and it is of general interest to understand how the protein accomplishes this. While X-ray diffraction provides important information in this regard, the resolution is insufficient to answer all questions. Especially important are questions involving the strength of hydrogen bonding interactions and electrostatic polarization. Relatively small distance changes between the heavy atoms involved in a hydrogen bond can cause mechanistically significant energy changes. Protein crystallographic studies are generally incapable of reliably detecting these effects or the important effects on substrate reactivity that the dipole moments and electrostatic fields of the protein contribute to enzyme action. However, such effects will alter the vibrational properties of the enzyme system, making vibrational spectroscopy an ideal method to complement the crystallographic analysis.

The early studies on the Raman spectroscopy of flavoproteins took advantage of the chromophoric nature of the isoalloxazine ring to generate intensity-enhanced resonance Raman spectra (*14; 15*). However, these efforts were severely hampered by fluorescence from the chromophore, and to avoid this, stratagems utilizing higher order Raman spectroscopies such as coherent anti-Stokes, or the inverse Raman effect, often had to be employed. These pioneering studies were technically difficult and could be carried out only in laboratories with expertise in advanced optical spectroscopy. However, recent technical progress promises to open the door to a more facile analysis of the Raman spectra of flavoproteins (*16; 17*). High-throughput spectrometers employing holographic supernotch filters and red-sensitive charge-coupled photon detectors provide Raman spectra with unprecedented sensitivity in the deep red region of the optical spectrum. The advantage of the latter, for example, using 752 nm excitation, is that no fluorescence is generated to swamp the Raman signal. We have undertaken a Raman spectroscopic study of PHBH, and report here our initial results which provide the foundation for dissecting the interactions between the protein, substrate, and prosthetic group in unprecedented detail. It is of note that the changes we observe in flavin Raman modes upon binding the substrate do not agree with those reported in an earlier study which used the inverse Raman effect (*18*) to record the Raman spectrum of the bound flavin. Reasons for these discrepancies are discussed, and these raise the possibility that some of the early Raman data for flavin-based systems may have to be reassessed.

MATERIALS AND METHODS

PHBH cloned from *Pseudomonas auerugenosa* was over expressed in *E. coli* (*19*) and purified by RedA affinity chromatography as previously described (*6*). *p*-Hydroxybenzoic acid and *p*-aminobenzoic acid were from Aldrich and were recrystallized from boiling water. *p*-Hydroxybenzoic acid labeled with ^{18}O in both carboxyl oxygens was prepared by heating at 110 °C in a sealed ampule with $H_2{}^{18}O$ (Cambridge Isotope Labs) and HCl as described (*20*). Mass spectral analysis showed ∼91% incorporation of two atoms of ^{18}O and ∼9% of 1 atom of ^{18}O in the product carboxyl group.

The concentrated PHBH solutions needed for Raman spectroscopy were prepared by precipitating the enzyme with ammonium sulfate (70% saturation) in 50 mM potassium phosphate buffer, pH 6.5. The precipitated enzyme was collected by centrifugation, and the semi-solid yellow material was transferred with a spatula to dialysis tubing. The ammonium sulfate-precipitated enzyme was dialyzed at 4 °C for about 12 h either against 6 L of the buffer desired for spectroscopy or against 10 mM Tris sulfate, pH 8.2. In the latter case, the desired pH was obtained immediately before spectra were collected by mixing the enzyme with aliquots of 1 M buffers at the desired pH. By these methods, PHBH solutions of up to 1.1 mM were obtained. The actual pH values of the solutions were measured after Raman spectra were collected.

In order to measure the pK_a of the unbound *p*OHB, a series of buffers were used to control the pH: pH 6.7−7.6, citrate−phosphate (0.1 M citric acid, 0.2 M dibasic sodium phosphate); pH 8.5−10.5, carbonate−bicarbonate (0.2 M sodium carbonate, 0.2 M sodium bicarbonate). The pH values were cross checked using two pH meters.

Raman spectra were acquired using a Spex 0.5 m single monochromator equipped with a CCD detector and a supernotch filter (*16*). Typically, 700 mW of 752 nm Kr^+ laser excitation was used with total exposure times of 15 min. Sample volumes of approximately 50 μL were used. In a typical experiment, the Raman spectrum of enzyme was recorded at 22 °C, and the spectrum of enzyme plus ligand was then recorded keeping conditions identical. The computer subtraction [enzyme + ligand] minus [enzyme] was then undertaken using Spectracalc software (Galactic Industries, Salem, NH).

RESULTS AND DISCUSSION

p-Aminobenzoate Binding to PHBH. *Para*-aminobenzoate is a competitive inhibitor of PHBH binding with an association constant of 5.0×10^4 M (*12*). The crystallographic structure of the complex has been solved at high resolution (2.2−2.0 Å) at pH values of 5.0, 7.4, 7.5, and 9.4 (*10; 12*). At the level of the crystallographic experiments, the structures of the *p*-amino- and *p*-hydroxybenzoate complexes are very similar. The carboxylate of both ligands is hydrogen-bonded to the guanidinium of Arg 214 and the hydroxyls of Ser 212 and Tyr 222. The *para* substituent of both ligands is involved in a hydrogen bond network with Tyr 201 and Tyr 385. The carbonyl of Pro 293 is also close enough to the *para* substituent of each ligand that it may also be involved in the hydrogen bond network. Though the hydrogens are invisible to protein crystallography, differences in the arrangement of protons in the hydrogen bond network have been inferred from molecular dynamics calculations (*12*).

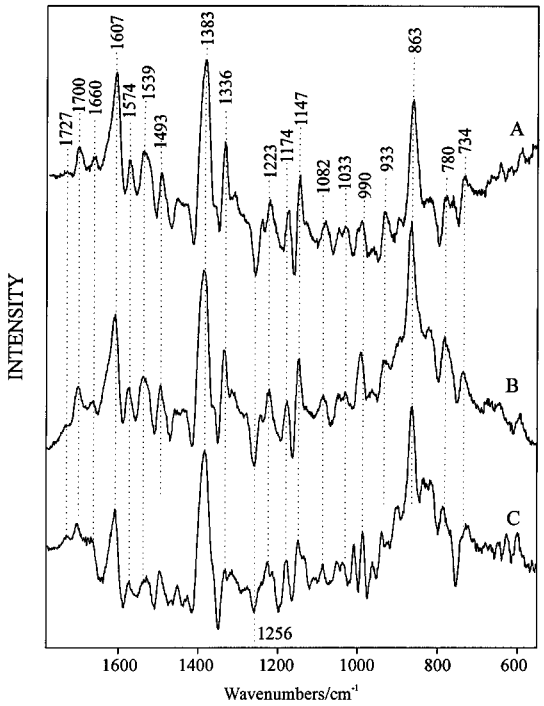

FIGURE 1: 752 nm excited Raman difference spectra of [*p*ABA bound to PHBH] minus [PHBH] in 50 mM phosphate, pH 6.49 (A), 50 mM phosphate, pH 7.49 (B), and 50 mM Tris−sulfate, pH 8.32 (C). The PHBH concentration was 0.96 mM in (A), 1.0 mM in (B), and 1.0 mM in (C).

For both ligands, the aromatic ring makes several contacts with hydrophobic protein side chains, such as Trp 185 and Leu 210, and is positioned near the N5−C6 area of the isoalloxazine moiety of the flavin. The *p*-aminobenzoate complex is a suitable place to begin the discussion of the Raman difference spectra of the complexes because the spectral interpretation is facilitated by the fact that the ligand does not undergo any protonation changes in the pH range of interest.

The Raman difference spectra of *p*-aminobenzoate (*p*ABA) bound to PHBH at pH 6.5, 7.5, and 8.3 are shown in Figure 1. The spectra are obtained by subtracting the 752 nm excited Raman spectrum of the enzyme from that of the enzyme−ligand complex. The first observation is that 752 nm excitation leads to high-quality Raman spectra free from interference from a luminescence background. Second, the spectra are very rich with many "positive" features (above the base line) and several "negative" features, with the combination of a negative and a positive peak sometimes giving rise to a derivative-type feature. Since the enzyme contains stoichiometric amounts of tightly bound FAD, the difference spectra [protein + FAD + *p*ABA] − [protein + FAD] can contain contributions from three sources, *viz.*, positive bands due to the bound *p*ABA, and features due to protein or FAD which can be positive and/or negative depending on how these entities are perturbed by binding of the *p*ABA. The Raman spectrum of *p*ABA is shown in Figure 2, and it is apparent that the three most intense ligand features, near 1610, 1385, and 860 cm^{-1}, dominate the difference spectra in Figure 1. These bands represent a phenyl ring mode (akin to the benzene 8a, 8b normal mode), the $-COO^-$ symmetric stretch, and a $-COO^-$ scissoring-like mode, respectively. Only the scissoring mode undergoes a small 6 cm^{-1} increase upon binding (Figures 1 and 2), showing that a major electron rearrangement in the ligand, and in the $-COO^-$ group in particular, does not occur upon

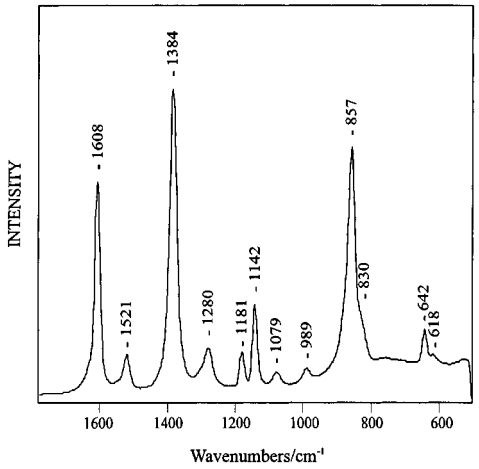

FIGURE 2: The 752 nm excited Raman difference spectrum of free *p*ABA, 0.1 M, at pH 6.5. The spectrum was obtained by subtracting the spectrum of buffer (phosphate) from the spectrum of *p*ABA in buffer.

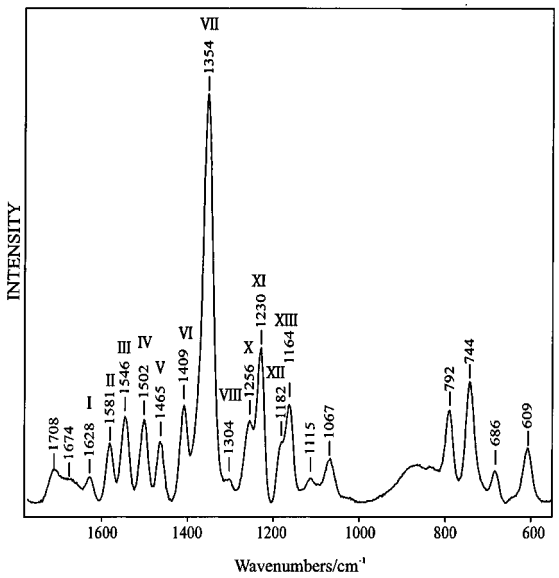

FIGURE 3: 752 nm excited Raman difference spectrum of 1 mM FAD in water at pH 5.65. The peaks are marked with Roman numerals in accordance with the convention of McFarland (*15*) and Morris and Bienstock (*14*).

binding. Furthermore, there is no evidence for any change in the *p*ABA modes in the complex in the pH range 6.5−8.5.

In our discussion of the flavin modes, we will use the notation for the ring modes that is set out in the reviews of McFarland (*15*) and Morris and Bienstock (*14*). Namely, the peaks from 1628 cm^{-1} to 1164 cm^{-1} are labeled from I to XIII as indicated in Figure 3. The assignment of features in the difference spectra in Figure 1 is more problematic but can be guided by a number of considerations:

(1) The isoalloxazine ring is a strong Raman scatterer, and any changes in the chemistry of the ring when *p*ABA is bound are expected to result in contributions from the isoalloxazine in the Raman difference spectra. The 752 nm excited Raman spectrum of FAD is shown in Figure 3, and the relatively high intensity of Raman peaks associated with the isoalloxazine is evinced by the fact that the 1100−1700 cm^{-1} region of Figure 3 is identical to the published Raman spectrum of riboflavin (which lacks the adenine nucleotide moiety) (*17*).

(2) If a feature (due to FAD, or a protein mode) changes in intensity, but not in frequency, upon *p*ABA binding, a positive or negative peak will result in the difference spectrum. With the convention for subtraction we are using, an increase in intensity in the ligand complex will result in a positive feature in the difference spectrum while a decrease in intensity will result in a negative feature.

(3) If a FAD or protein feature undergoes a small (0−10 cm^{-1}) frequency shift upon *p*ABA binding, the resulting trace in the difference spectrum will have the appearance of a derivative peak.

One difficulty in interpreting the spectra in Figure 1 is that in many regions it is difficult to define the base line with certainty because of overlapping "positive" and "negative" features. However, there are some regions of the spectrum that can be assigned with confidence. The "positive" features seen in Figure 1 at 1574, 1539, and 1493 cm^{-1} are almost certainly associated with modes II, III, and IV identified in Figure 3. They may, in fact, be more derivative in character than simple positive features since the peak maxima in Figure 1 have shifted significantly from the positions in free FAD (Figure 3). The changes in peak positions are evidence that a change in the hydrogen bonding contacts about the flavin ring (at the C2═O-N3H-C4═O region) is occurring upon binding the *p*ABA (*14*, *15*). This conclusion is supported by the negative feature at 1256 cm^{-1} (Figure 1) which is due to a diminution of the intensity of isoalloxazine band XI when the *p*ABA binds. Changes in band XI are also diagnostic for perturbations in the hydrogen bonding structure about the C4−C6 region (*21*, p 142). Elsewhere in the spectra in Figure 1, the derivative feature with its positive arm at 1336 cm^{-1} connotes a small downward shift of the intense band VII mode. Some other features, for example, at 792 and 686 cm^{-1}, may be associated with isoalloxazine bands seen in Figure 1. However, several bands in the spectra, e.g., between 990 and 1040 cm^{-1}, are almost certainly not flavin or *p*ABA modes and must be due to changes in protein groups upon ligand binding. Likely candidates that can be identified from the crystal structure include Trp 185, Tyr 201, Tyr 222, and Tyr 385, each of which is in close proximity to the aromatic ligand in the enzyme−substrate complex. There is obviously a rich area for future study.

One part of the spectrum that is more accessible is the 1700 cm^{-1} region, where we expect the isoalloxazine C═O stretching features to occur (*17*). For FAD in aqueous solution (Figure 3), the broad band at 1708 cm^{-1} can be assigned to a mode which has a high degree of C4═O stretching character (*17* and refs *6*, *7*, *8* therein). The unresolved band near 1674 cm^{-1} may be assigned tentatively to C2═O stretch. However, both the C═O assignments and the possible degrees of vibrational coupling between the two groups need to be explored by isotopic substitutions. The C═O bands appear in the enzyme difference spectra at 1700 and 1660 cm^{-1} (Figure 1), indicating that the carbonyls are in a well-defined hydrogen bonding environment in the enzyme/FAD/*p*ABA complex, where the strength of the hydrogen bonding is slightly greater than that for the free C═Os exposed to water in Figure 3. The facts that the C═Os appear as sharp positive features in the difference spectra in Figure 1 and that there are no discernible negative peaks suggest that in the FAD environment in the protein, without *p*ABA present, the flavin carbonyls are "washed out" by a fluctuating series of hydrogen bonds to water molecules which penetrate to the flavin ring, resulting in broad C═O features which escape detection in the difference spectra. When the *p*ABA is present, most solvent molecules are expelled, and the carbonyls are held in an essentially rigid environment. The X-ray data, shown in Figure 4, show that C4═O has two, and C2═O three, putative hydrogen bonding contacts. This results in sharp well-defined C═O peaks which are recognized in the positive direction in the difference spectra in Figure 1.

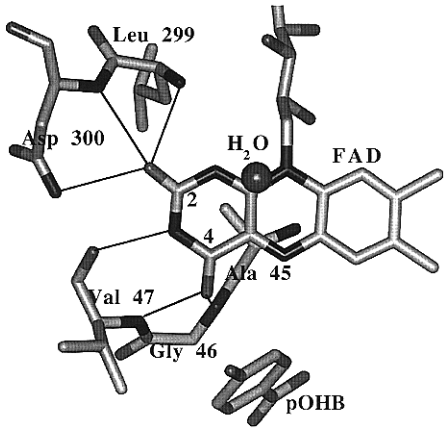

FIGURE 4: Hydrogen bonds to the isoalloxazine moiety in the active site of PHBH. Possible hydrogen bonds (as judged by distance) between protein residues and the pyrimidine end of the isoalloxazine are shown as solid lines. The 2- and 4-carbons of the flavin are labeled with numerals. Coordinates are from Schreuder et al. (1989) (*7*).

A final conclusion to be drawn from Figure 1 is that there is evidence for a pH-dependent change in the complex between pHs 7.5 and 8.3. For example, a substantial change occurs in the ratio of the intensities of the carbonyl peaks at 1727 and 1700 cm^{-1}, and there are many other discernible changes in the difference traces for flavin and protein features between pH 7.5 and 8.3. Thus, it can be said that the change, brought about by side chain ionization(s), involves both the environment of the flavin ring system and groups or parts of the protein. It should be possible in future studies to assign these spectral features by using appropriate site-directed mutants and isotopically substituted flavins.

p-Hydroxybenzoate Binding to PHBH. The 752 nm excited Raman difference spectra of *p*-hydroxybenzoate (*p*OHB) bound to PHBH are shown in Figure 5 at pH values of 6.5, 7.5, 8.3, and 9.2. Within this pH range, the substrate loses a proton to give the doubly ionized form $-O^-$, $-COO^-$. The ionization of the hydroxyl group for the bound ligand has been measured by absorption difference spectroscopy and assigned a pK_a value of 7.4 (*3*). This compares with a pK_a of 8.9 for the free ligand (see next section). The lowering of the pK_a is thought to assist catalysis by favoring the phenolate form of *p*OHB. The increased electron density at the 3-position of the phenolate makes it a more reactive nucleophile in the oxygen-transfer reaction with the enzyme-bound flavin hydroperoxide (*4*). The measurement of the pK_a using the Raman data and ^{18}O-labeled *p*OHB will be discussed in the next section. Here we shall make some general observations based on the difference data shown in Figure 5 and a comparison with the foregoing discussion on the *p*-amino analog.

The Raman spectra of *p*OHB, in aqueous solution, in its singly (pH 6.5) and doubly (pH 11.7) ionized forms, are presented in Figure 6. The major spectral change upon

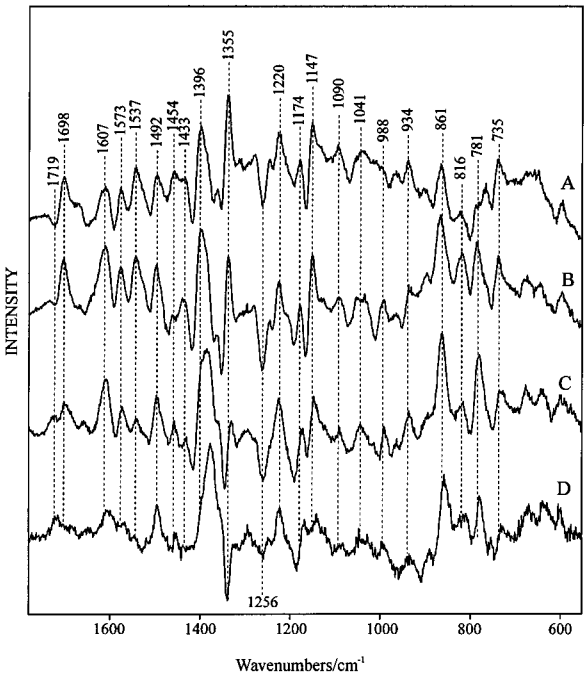

FIGURE 5: 752 nm excited Raman difference spectra of substrate, *p*OHB (1 mM), bound to PHBH (1 mM) in 50 mM phosphate, pH 6.49 (A), 50 mM phosphate, pH 7.49 (B), 50 mM Tris−sulfate, pH 8.32 (C), and 50 mM glycine, pH 9.25 (D).

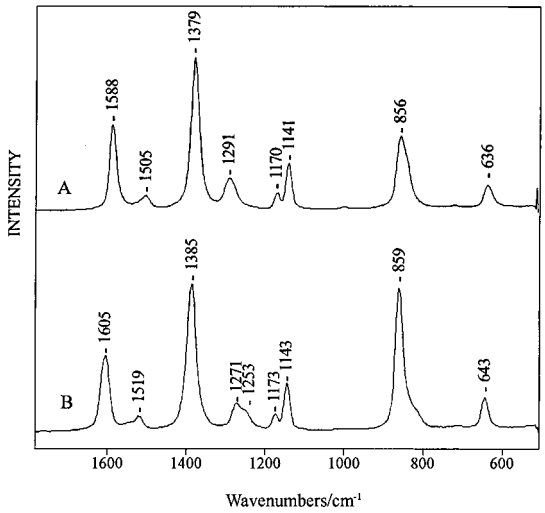

FIGURE 6: 752 nm excited Raman spectra of ~0.1 M *p*OHB in its singly (pH adjusted to 6.5 with NaOH) (B) and doubly ionized (pH adjusted to 11.7 with NaOH) forms in aqueous solution (A).

ionization of the −OH group is in the ratio of the intensities of the $-COO^-$ scissoring mode near 860 cm^{-1} and the $-COO^-$ symmetric stretch near 1380 cm^{-1}. This change will be used in the next section to measure the pK_a for the ionization, for both the free and PHBH-bound ligand.

In the Raman difference spectrum of the complex at pH 6.5 (Figure 5A), the features due to the substrate near 1605, 1390, and 860 cm^{-1} are of lesser relative intensity compared to the *p*ABA peaks seen in Figure 1. This is because the pOHB has a lower Raman cross section than *p*ABA by approximately a factor of 2 (unpublished work, this laboratory). In contrast to the *p*ABA complex, the $-COO^-$ symmetric stretch shifts 10 cm^{-1} to 1396 cm^{-1}. This shift we ascribe to the salt bridge, identified by crystallographic studies, between the $-COO^-$ and the guanidinium of arginine 214. Since no change in frequency is seen for the *p*ABA complex, it is likely that the guanidinium/$-COO^-$ interaction is weaker therein. Such a difference cannot be detected in the X-ray crystallographic data for the *p*ABA and *p*OHB complexes, and this points to the advantage of vibrational spectroscopy for elucidating the fine details of structure and electron redistribution.

Overall, there is a broad similarity between the flavin and protein features in the difference spectra of the *p*OHB and *p*ABA complexes, and this similarity extends to the response to a change in pH. For example, the spectral changes between 700 and 850 cm^{-1}, seen in Figure 5 going from pH 6.5 to 7.5, are essentially mirrored in Figure 1. The appearance of peaks near 1573, 1537, and 1492 cm^{-1} is very similar, as is the negative feature near 1258 cm^{-1}. Thus, as in the case of the *p*ABA complex, we ascribe these changes to a change in the hydrogen bonding environment about the flavin ring system with the isoalloxazine being held in the well-ordered network of hydrogen bonds seen in Figure 4. The marked similarities of the foregoing features in the spectra of the substrate and substrate analog give us confidence in the reproducibility of our Raman difference data. However, our conclusions are at variance with those of Bienstock, Schopfer, and Morris (*18*). These authors used resonance inverse Raman spectroscopy to probe changes in flavin bands in PHBH when binding a number of ligands, including the substrate *p*OHB. For the latter experiment, Bienstock et al. reported that substrate binding perturbed the positions of bands VI and V (Figure 3) but few changes could be observed elsewhere and, in particular, the 1400 −1600 cm^{-1} region of the spectrum was unaltered by substrate binding. This contrasts sharply with our conclusions. A possible reason for the discrepancy is the difference in techniques. We are undertaking normal, continuous-wave Raman spectroscopy with a wavelength far from any chromophore absorption band. In contrast, Bienstock et al. used one cw wavelength in resonance with the flavin chromophore and also pumped with intense near-UV pulses. The possibility exists that they were promoting a photochemical reaction, such as the well-known flavin photoreduction. If that were so, then their spectra, which were obtained in an aerobic environment, could be a combination of the spectra of the several enzyme forms that would be present during light-driven turnover. Alternatively, our assignments of features in the Raman difference spectra in the 1500 cm^{-1} region (Figures 1 and 5) to flavin bands II, III, IV, and V may be incorrect. This issue will be resolved in a future publication.

The comparison for the *p*ABA and *p*OHB complexes in the carbonyl spectral region is interesting. In Figure 5A, there is evidence for a negative feature near 1719 cm^{-1} as well as a positive peak near 1698 cm^{-1}. This suggests that a flavin carbonyl in the unliganded enzyme occurs near 1720 cm^{-1}, which is the position expected for C4═O exposed to water (*17*). Upon binding of the substrate, this feature appears to be replaced by a well-defined C═O stretch near 1700 cm^{-1}. These data support the interpretation given for the *p*ABA complex, *viz.*, that prior to binding of the substrate the C2−C4 region of the isoalloxazine ring is exposed to solvent molecules which gives rise to a broad C4═O feature near 1720 cm^{-1}. (The failure to detect a negative feature near 1720 cm^{-1} in Figure 1 may simply reflect the poorer signal-to-noise ratio compared to Figure 5.) Upon binding the substrate or a substrate analog, the solvent no longer has access to this region of the flavin ring system which is now held as shown in Figure 4. The hydrogen bonds to C4═O

decrease its frequency and result in a "sharper", better defined spectral profile. This interpretation is consistent with the available structural data. A high-quality structure of ligand-free PHBH is unavailable because diffraction-quality crystals seem to require a ligand bound to the active site. However, a low-resolution structure of ligand-free PHBH has been described (*22*). In the absence of an aromatic ligand, the binding pocket appears to be occupied by two water molecules which are involved in an array of hydrogen bonds with the isoalloxazine and the three active site tyrosines (201, 222, and 385). Furthermore, the positions of the tyrosine inferred from the electron density indicate that these residues have moved compared to their positions in enzyme−ligand complexes. The relatively poor quality of the ligand-free structure makes detailed interpretation unreliable. However, the difficulty in collecting high-quality diffraction data and the inability to grow high-quality crystals without an aromatic ligand are consistent with the notion that the ligand-free enzyme is in a more fluctional state than PHBH−ligand complexes.

Throughout the difference spectra in Figure 5, there is clear evidence for variations occurring with changes in pH. There are two sources giving rise to the observed changes. One is an ionization of protein side chain(s), known to perturb the Raman difference features from the flavin ring and the protein (Figure 1). The second source is ionization of the substrate's −OH group. Since knowledge of the pK_a of the latter is of mechanistic import, we undertook experiments with ^{18}O labeling of the $-COO^-$ group in order to probe the behavior of the substrate unencumbered by interference from protein groups. In Figure 5, it is noteworthy that a major change in band V's difference intensity (at 1355 cm^{-1}) occurs with pH, whereas corresponding behavior cannot be detected in Figure 1. These changes may be reflecting the ionization of the substrate's −OH group, although due to the complex nature of the band profiles near 1355 cm^{-1} it would be difficult to use this region to determine a pK_a for the *p*-hydroxyl group.

Using ^{18}O-Labeled Substrate To Follow Ionization of the −OH Group. As we have already seen in Figure 6, ionization of the substrate's −OH group results in a large change in the relative intensities of the dominant Raman features, the $-COO^-$ symmetric stretch, and scissoring modes near 1380 and 860 cm^{-1}, respectively. In order to follow the ionization for the bound substrate, our strategy is to subtract the Raman spectra of the unlabeled enzyme−substrate complex from those of the complex where the substrate's $-COO^-$ group is fully labeled with ^{18}O. In this way, the only normal modes appearing in the difference spectrum are those which involve the motion of the oxygens of the acid group, allowing the relative intensities of the 1380 and 860 cm^{-1} features to be used to measure the pK_a. Initially we used this approach to compare the pK_a for the free substrate derived by Raman spectroscopy with that derived by absorption spectrophotometry.

For the substrate in aqueous solution, when the $-COO^-$ group is fully labeled with ^{18}O, the peaks for the singly ionized molecule seen in Figure 6 at 859, 1143 and 1385 cm^{-1} shift to 850, 1131, and 1366 cm^{-1}, respectively. As a result, subtraction of the Raman spectrum of the ^{18}O-labeled substrate from that of the unlabeled substrate at exactly the same concentration yields the trace seen in Figure 7. In order to measure the pK_a for ionization of the −OH group, the ratios of the distances from the derivative maxima and minima at about 860 and 1380 cm^{-1}were measured as a function of pH for a series consisting of matched pairs of labeled and unlabeled substrates, each pair being at the same pH and concentration. Thus, in Figure 8, the ordinate, the "ratio of derivatives" axis, corresponds to the distance between the maxima and minima points near 1380 cm^{-1}, seen in Figure 7, divided by the distance between the maxima and minima points near 860 cm^{-1}. Figure 8 shows that the pK_a derived by this method is identical to that measured by changes in absorbance at 280 nm. Both methods show an apparent pK_a for the −OH group of the aqueous substrate of 8.9. This value is slightly lower than the value of 9.31 reported in the literature (*23*) because we did not extrapolate our results to zero ionic strength.

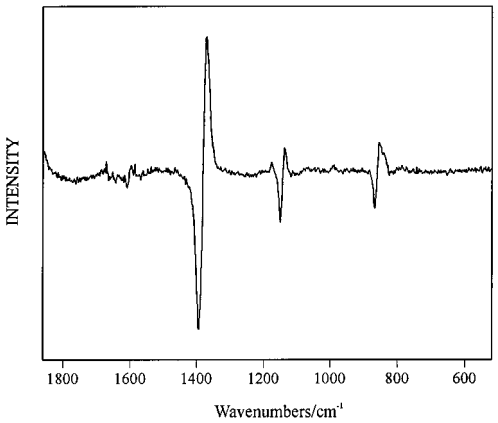

FIGURE 7: 752 nm excited Raman difference spectrum of $-C^{18}O^{18}O$ labeled *p*OHB from unlabeled *p*OHB, pH 6.7, 6.6 mM.

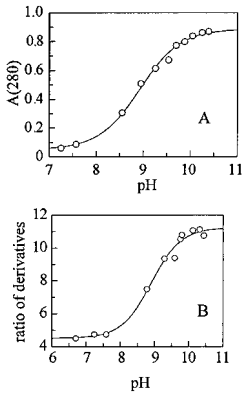

FIGURE 8: Comparison of pK_a values of unbound *p*OHB derived by monitoring the absorbance at 280 nm (A) and by taking the ratio of the amplitudes of the Raman derivatives near 1380 and 860 cm^{-1} resulting from the $-C^{18}O^{18}O$-labeled *p*OHB minus unlabeled subtraction (B).

The same approach was used to obtain difference spectra of the ^{18}O-labeled and unlabeled substrate bound to PHBH. A difference spectrum for a matched pair is shown in Figure 9. The difference spectrum has the same general appearance as that for the free ligand; however, the signal-to-noise ratio is poorer, and the ratios of peak intensities are different for the bound and free ligand, reflecting the different environments about *p*OHB in the two cases. Measurements at different pH values gave the curve shown in Figure 10. Although reliable data could not be collected above pH 9 due to enzyme denaturation, the points in Figure 10 were fit using GraFit to yield a pK_a value of 8.3. This compares to the value of 8.9 for the free ligand and to the value of 7.4 for the bound *p*OHB derived by absorption spectroscopy (*3*). For comparison purposes, a theoretical curve for a pK_a of

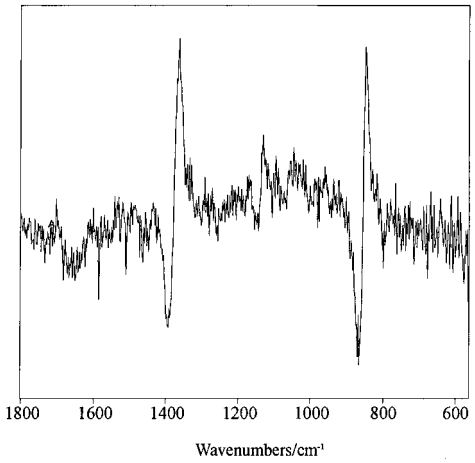

FIGURE 9: 752 nm excited Raman difference spectrum of $-C^{18}O^{18}O-$ labeled and unlabeled *p*OHB bound to PHBH, pH 6.3, 1.0 mM.

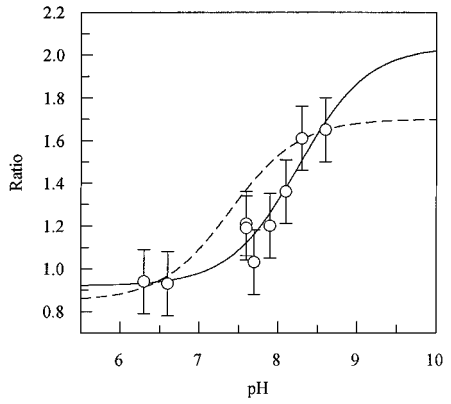

FIGURE 10: Ratio of the amplitudes of the Raman derivatives for the difference spectra, as seen in Figure 9, as a function of pH, for bound substrate *p*OHB. The solid curve represents a least-squares fit to the data giving a p*K* of 8.3. The dashed curve represents a fit with the pK_a fixed to a value of 7.4.

7.4 appears as a dashed line in Figure 10. Thus, while both the absorption and Raman measurements indicate that the PHBH active site lowers the pK_a of the −OH of the substrate substantially, the two techniques are in quantitative disagreement by 0.9 of a pH unit. There are a number of possible sources for the discrepancy. The value derived from absorbance measurements could conceivably include contributions from chromophores other than *p*OHB leading to an observed pK_a depending on more than one ionizing group. However, no such ionization was observed in studies of the Tyr201Phe mutant (*3*), the Tyr385Phe mutant (*5*), or the Asn300Asp mutant (*6*). None of these mutant enzymes lowers the pK_a of *p*OHB as determined by absorbance spectroscopy, and in the absence of substrate ionization, no other chromophore contributes a pH-dependent absorbance change in the region of 290 nm. We can see from the Raman difference measurements for bound *p*ABA in Figure 1 that ionizations of protein groups in the pH range 6.5−8.5 bring about changes to difference features due to the flavin ring and protein modes. It is conceivable that such ionizations also perturb the absorbance and Raman spectral properties of *p*OHB in a differential manner, thus affecting the measured pK_a values. A major limitation of the Raman measurements is the low signal-to-noise ratio we have achieved in the difference spectra, as seen in Figure 9 . This drawback can be addressed in the near future because new technologies in spectrometer design and improvements in photon detectors will increase the S/N ratios by at least a factor of 3. At this time, we can say that both Raman and absorption spectroscopies provide evidence for a substantial lowering of the substrate's −OH pK_a upon binding. As the new Raman technologies become available, we intend to improve the quality of the Raman difference measurements and obtain a more accurate measurement of the "Raman" pK_a.

ACKNOWLEDGMENT

The help of Dr. Jian Dong (Case Western Reserve University) in measuring the relative Raman cross sections of *p*OHB and *p*ABA, Mr. Alfio Zappala (Case Western Reserve University) in measuring the pK_a of free *p*OHB, and Ms. Mariliz Ortiz-Maldonado (University of Michigan) in preparing enzyme is gratefully acknowledged.

REFERENCES

1. Entsch, B., and van Berkel, W. J. H. (1995) *FASEB J. 9*, 476−483.
2. Shoun, H., Arima, K., and Beppu, T. (1983) *J. Biochem. 93*, 169−176.
3. Entsch, B., Palfey, B. A., Ballou, D. P., and Massey, V. (1991) *J. Biol. Chem. 266*, 17341−17349.
4. Vervoort, J., and Reitjens, I. M. (1996) *Biochem. Soc. Trans. 24*, 127−130.
5. Eschrich, K., van der Bolt, F., de Kok, A., and van Berkel, W. J. H. (1993) *Eur. J. Biochem. 216*, 137−146.
6. Palfey, B. A., Entsch, B., Ballou, D. P., and Massey, V. (1994) *Biochemistry 33*, 1545−1554.
7. Schreuder, H. A., Prick, P. A. J., Wierenga, R. K., Vriend, G., Wilson, K. S., Hol, W. G. J., and Drenth, J. (1989) *J. Mol. Biol. 208*, 679−696.
8. Schreuder, H. A., van der Laan, J. M., Swarte, M. B. A., Kalk, K. H., Hol, W. G. J., and Drenth, J. (1992) *Protein: Struct., Funct., Genet. 14*, 178−190.
9. Lah, M. S., Palfey, B. A., Schreuder, H. A., and Ludwig, M. L. (1994) *Biochemistry 33*, 1555−1564.
10. Schreuder, H. A., Mattevi, A., Obmolova, G., Kalk, K. H., Hol, W. G. J., van der Bolt, F. J. T., and van Berkel, W. J. H. (1994) *Biochemistry 33*, 10161−10170.
11. Gatti, D. L., Palfey, B. A., Lah, M. S., Entsch, B., Massey, V., Ballou, D. P., and Ludwig, M. L. (1994) *Science 266*, 110−114.
12. Gatti, D. L., Entsch, B., Ballou, D. P., and Ludwig, M. L.-(1996) *Biochemistry 35*, 567−578.
13. Schreuder, H. A., Hol, W. G. J., and Drenth, J. (1990) *Biochemistry 29*, 3101−3108.
14. Morris, M. D., and Bienstock, R. J. (1986) in *Spectroscopy of Biological Systems* (Clark, R. J. H., & Hester, R. E., Eds.) Chapter 8, J. Wiley, Chichester.
15. McFarland, J. T. (1987) in *Biological Applications of Raman Spectroscopy* (Spiro, T. G., Ed.) Vol. 2, Chapter 5, Wiley Interscience, New York.
16. Kim, M., Owen, H., and Carey, P. R. (1993) *Appl. Spectrosc. 47*, 1780−1783.
17. Kim, M., and Carey, P. R. (1993) *J. Am. Chem. Soc. 115*, 7015−7016.
18. Bienstock, R. J., Schopfer, L. M., and Morris, M. D. (1986) *J. Am. Chem. Soc. 108*, 1833−1838.
19. Moran, G. R., and Entsch, B. (1995) *Protein Expression Purif. 6* , 164−168.
20. Orville, A. M., Harpel, M. R., and Lipscomb, J. D. (1990) *Methods Enzymol. 188*, 107−115.
21. Carey, P. R. (1982) *Biochemical Applications of Raman and Resonance Raman Spectroscopies*, Academic Press, New York.
22. van der Laan, J. M. (1986) Doctoral Thesis, University of Groningen.
23. Matto, B. N. (1956) *Trans. Faraday Soc. 52*, 1462−1465.

BI9715270